Antitumor effect of humanized anti-tissue factor antibody-drug conjugate in a model of peritoneal disseminated pancreatic cancer

RYO TSUMURA[1], TAKAHIRO ANZAI[1], SHINO MANABE[2,3], HIROKI TAKASHIMA[1], YOSHIKATSU KOGA[1], MASAHIRO YASUNAGA[1] and YASUHIRO MATSUMURA[4]

[1]Division of Developmental Therapeutics, EPOC, National Cancer Center, Kashiwanoha, Kashiwa, Chiba 277-8577; [2]Laboratory of Functional Molecule Chemistry, Pharmaceutical Department and Institute of Medicinal Chemistry, Hoshi University, Ebara, Shinagawa, Tokyo 142-8501; [3]Research Center for Pharmaceutical Development, Graduate School of Pharmaceutical Sciences and Faculty of Pharmaceutical Sciences, Tohoku University, Aoba, Aramaki, Aoba-ku, Sendai, Miyagi 980-8578; [4]Department of Immune Medicine, National Cancer Center Research Institute, Tsukiji, Chuo-ku, Tokyo 104-0045, Japan

Received June 30, 2020; Accepted October 13, 2020

DOI: 10.3892/or.2020.7850

Abstract. Tissue factor (TF) is an attractive target for cancer therapy due to its overexpression in multiple types of malignancies. In addition, TF has been reported to play functional roles in both cancer development and metastasis. Several groups have already developed antibody-drug conjugates (ADCs) against TF for use as cancer treatments, and have demonstrated their efficacies in conventional subcutaneous xenograft models and patient-derived xenograft models. However, no previous studies have investigated the effectiveness of anti-TF ADC in an advanced-stage cancer model. The present study developed an original humanized anti-TF monoclonal antibody conjugated with monomethyl auristatin E, and evaluated its *in vivo* efficacy in a pancreatic cancer xenograft model with peritoneal dissemination. *In vitro* assays demonstrated that the anti-TF ADC had potent binding affinity and cytotoxic activity against human pancreatic cancer cells that strongly expressed TF antigens. The anti-TF ADC also exhibited greater antitumor effect than that of a control ADC in conventional subcutaneous xenograft models, with efficacy depending on the TF expression in the tumor tissues. Furthermore, the anti-TF ADC significantly inhibited tumor growth in an orthotopic xenograft model, and extended the survival period in a murine peritoneal dissemination model. These results indicated that anti-TF ADC has the potential to be an effective treatment not only for primary tumors, but also for those that are widely disseminated. Therefore, it can be concluded that ADC targeting TF may be a promising agent for advanced pancreatic cancer therapy.

Correspondence to: Dr Yasuhiro Matsumura, Department of Immune Medicine, National Cancer Center Research Institute, 5-1-1 Tsukiji, Chuo-ku, Tokyo 104-0045, Japan
E-mail: yhmatsum@ncc.go.jp

Key words: antibody-drug conjugates, antitumor effects, pancreatic cancer, peritoneal dissemination, tissue factor

Introduction

Pancreatic cancer has the worst prognosis among all malignancies. The 5-year survival rate of patients with pancreatic cancer is 8% despite advances in treatment (1). The majority of patients with pancreatic cancer have distant metastasis and peritoneal dissemination at the time of diagnosis (2), and therefore most are unable to undergo curative surgical treatment (3). As a result, the development of effective chemotherapy regimens is extremely important for this population.

Tissue factor (TF), a 47-kDa transmembrane glycoprotein, is widely known to play a role in initiating the extrinsic blood coagulation cascade. The correlation between blood coagulation and cancer has been extensively discussed (4-6). Invasion of cancer cells, enhanced vascular permeability and abnormal inflammation can trigger hyper-coagulation in tumor tissues (7). In fact, TF overexpression has been observed in various cancer types, including pancreatic cancer (8-10). In addition to its role in initiating the blood coagulation cascade, TF plays functional roles in cancer development, for instance in the areas of tumor growth, inflammation, and angiogenesis (11). Recently, several studies reported that TF expression was also correlated with tumor metastasis in several cancer types (12-15). Other studies demonstrated that the downregulation of TF expression in cancer cells and the blockade of TF by anti-TF monoclonal antibodies inhibited tumor metastasis *in vivo* (12,16,17). Thus, TF may be an ideal target for cancer treatments.

The use of antibody-drug conjugates (ADCs) is currently considered to be a powerful strategy in cancer therapy. ADCs have three components, namely a monoclonal antibody (mAb), a potent payload, and a linker. The antigens on cancer cell membranes are typical targets of ADCs.

When these antigens are endocytosed, the bound ADCs are internalized into the cancer cells, and the linker is then selectively cleaved by proteases such as cathepsin B in lysosomes. This cleavage of the linker causes the release of the anticancer agents into the cytoplasm, thus inducing cell apoptosis. Anti-TF ADCs have been investigated in several studies (17-23). The efficacy of these agents was confirmed using various animal models (including conventional subcutaneous xenograft models, patient-derived xenograft models and mouse orthotopic models) and in various cancer types (such as pancreatic, lung, prostate, ovarian, bladder, and breast cancer, and cervical squamous cell carcinoma). One of these anti-TF ADCs, tisotumab vedotin, is currently in clinical trials, which has demonstrated clinical responses in patients with recurrent or metastatic cervical cancer (24,25). In the majority of cases, ADCs are employed for the treatment of advanced cancer with metastasis. However, few basic studies have investigated the efficacy of anti-TF ADCs in advanced-stage cancer models such as abdominal dissemination or distant metastasis.

In the present study, a humanized anti-TF antibody was constructed, and its binding specificity was confirmed. Previous studies demonstrated that the bis-alkylating conjugation strategy was more feasible than the conventional maleimide-based conjugation strategy for ADC construction (23,26,27). Therefore, the bis-alkylating bis-sulfone group-PEG12-valine-citrulline-*p*-amino-benzoyloxycarbonyl (bisAlk-PEG12-vc-PABC) linker and monomethyl auristatin E (MMAE) were used in the preparation of the humanized anti-TF ADC, and its efficacy was evaluated in several pancreatic cancer models, including the orthotopic model and peritoneal dissemination model.

Materials and methods

Generation of humanized anti-TF monoclonal antibody. Rat anti-TF mAb (clone 1084) was humanized as previously described (28). Briefly, the complementarity-determining regions of rat anti-TF mAb were grafted onto a human antibody framework (IgG1). The procedure was performed according to standard humanization protocols (29). The heavy chain and the kappa light chain cDNAs were cloned into a pcDNA3.3 expression vector (Thermo Fisher Scientific, Inc.). These expression vectors were transiently transfected into ExpiCHO cells (Thermo Fisher Scientific, Inc.) according to the manufacturer's protocol.

Cell cultures. BxPC-3, HPAF-II, PSN-1 and Panc-1 cells were obtained from the American Type Culture Collection (ATCC, Manassas, VA, USA), while Suit-2 cells were obtained from the Japanese Collection of Research Bioresources (JCRB, Tsukuba, Japan). To evaluate the efficacy of anti-TF ADC *in vivo*, the CRISPR-Cas9 system was used to generate BxPC-3 TF knock-out cells (BxPC-3-TF-KO), and the CMV-GFP-T2A-Luciferase Lentivector system (System Biosciences) was used to produce HPAF-II cells that stably expressed firefly luciferase (HPAF-II-Luc). These cell lines were cultured in ATCC- or JCRB-recommended medium supplemented with 10% fetal bovine serum (FBS, Thermo Fisher Scientific, Inc.), penicillin G (100 units/ml), streptomycin (100 μg/ml), and amphotericin B (0.25 μg/ml; FUJIFILM Wako Pure Chemical Corp.) in a 5% CO_2 atmosphere at 37˚C.

Preparation of ADC. The ADC preparation protocol was previously described (23). The bisAlk-PEG12-vc-PABC linker was used for conjugation with MMAE to humanized control mAb or humanized anti-TF mAb. The mAbs were reduced by 35 mM 1,4-dithiothreitol (Sigma Aldrich; Merck KGaA), and then reacted with the linker at 4˚C overnight. After the unreacted linker was removed, ADCs were stored at -80˚C until use in subsequent experiments.

Determination of molecular particle size. To estimate the molecular sizes of mAbs and ADCs, particle size analysis was performed using DelsaNano HC (Beckman Coulter) based on photon correlation spectroscopy (PCS) and dynamic light scattering (DLS), as previously described (30). Briefly, the particle size of each mAb and ADC was measured by DelsaNano HC after the protein concentration was adjusted to 1 mg/ml.

ELISA. The ELISA procedure was previously described (22). Briefly, recombinant human TF and mouse TF antigens were immobilized on C8 MaxiSorp plates (Thermo Fisher Scientific, Inc.). Antibodies and ADCs were applied at each concentration and left to react for 15 min at room temperature (RT) (n=3). As a secondary antibody, goat anti-human (H+L) pAb-HRP (Medical & Biological Laboratories Co., Ltd.) was then allowed to react for 15 min at RT. The absorbance was determined with a SpectraMax190 microplate reader (Molecular Devices, LLC).

Flow cytometry (FCM) analysis. The FCM procedure was performed as previously described (23). To detect human TF antigens, goat anti-human TF polyclonal antibody (R&D Systems) and anti-goat IgG (H+L) cross-adsorbed secondary antibody conjugated with Alexa Fluor 647 (Thermo Fisher Scientific, Inc.) were used. A Guava easyCyte flow cytometer (Merck Millipore) and FlowJo analysis software (v10.6.1; Tree Star Inc.) were used to analyze the data.

Assessment of cell cytotoxicity in vitro. The cytotoxicity assessment procedure was previously described (22). BxPC-3, BxPC-3-TF-KO and HPAF-II cells were harvested on 96-well plates (Corning) and incubated at 37˚C overnight. MMAE and ADCs were applied at each concentration, and the plates were incubated at 37˚C for 72 h. MMAE was applied at the same concentrations with the payloads conjugated with ADC. Cell Counting Kit-8 (Dojindo Molecular Technologies) was used to evaluate cell viability (n=3).

Animal models. A total of 125 female BALB/c nude mice (Charles River Laboratories Japan, five-week-old, initial average weight 20.6 g) were used in the subsequent experiments. The mice were maintained in cages under specific pathogen-free condition (temperature; 23˚C, humidity; 50%) and exposed to a 12-h light/dark cycle. Sterilized water and standard food were offered *ad libitum*. In all experiments, mice were anesthetized by inhalation with 1-2% isoflurane (Pfizer). To prepare the subcutaneous tumor models, $2x10^6$ BxPC-3, BxPC-3-TF-KO

or HPAF-II cells were subcutaneously implanted into mice under deep anesthesia. Tumor volume was calculated by the following formula: Volume=length x (width)^2 x 1/2. To prepare the orthotopic tumor model, 1x10^6 HPAF-II cells were injected into the pancreas of mice under deep anesthesia. To prepare the peritoneal dissemination model, 1x10^6 HPAF-II-Luc cells were intraperitoneally injected into mice under deep anesthesia. Tumor volume exceeding 2,000 mm^3, weight loss of 20% or more, ascites retention, and apparent reduction in physical activity were set as humane endpoints. As a method of euthanasia, mice were euthanized by cervical dislocation after confirming that they were sufficiently anesthetized by halation with isoflurane.

Antitumor effects in the subcutaneous and orthotopic tumor models. In the subcutaneous tumor model, the treatment was started when the tumor volume reached approximately 200 mm^3. In the BxPC-3 xenograft model, mice (n=5) underwent three weekly treatments with intravenous DPBS, humanized anti-TF mAb (10 mg/kg), humanized control ADC (10 mg/kg), or humanized anti-TF ADC (2, 5 and 10 mg/kg). In the HPAF-II and BxPC-3-TF-KO xenograft models, mice (n=5) received three weekly treatments with DPBS or each ADC (10 mg/kg).

In the orthotopic tumor model, the treatment was started 3 weeks after transplantation. The mice (n=8) were administered intravenous DPBS, humanized control ADC (10 mg/kg), or humanized anti-TF ADC (10 mg/kg) once a week for 4 weeks. After treatment, the mice were sacrificed under deep anesthesia. The tumors were harvested and their weights were measured.

Antitumor effects in the peritoneal dissemination model. In the peritoneal dissemination model, the treatment was started 2 weeks after transplantation (Day 0). *In vivo* photon counting analysis was performed using the IVIS kinetic imaging system (Caliper Life Sciences) and IVIS Living Imaging 3.0 software (Caliper Life Sciences) at Day 0, 14, and 28. At Day 0, the mice were randomly grouped based on bioluminescence intensity in the regions of interest (ROIs) in the abdominal area. The average bioluminescence intensity was approximately 5.0-5.5x10^6 photons/sec at Day 0. The mice (n=11) were treated weekly with intravenous DPBS, humanized control ADC (10 mg/kg) or humanized anti-TF ADC (10 mg/kg) for 4 weeks. The bodyweight and mortality were checked twice or thrice per week. In the survival study, the mice were sacrificed when weight loss of 20% or more, ascites retention, and apparent reduction in physical activity were observed. In addition, the monitoring period was set to 4 months because the survival period of this model was 1-2 months in a preliminary study.

All animal experiments were carried out with the approval of the Committee for Animal Experimentation of the National Cancer Center, Japan. Experiments met the ethical standards required by law and also complied with guidelines for the use of experimental animals in Japan.

Statistical analysis. Statistical analysis was conducted using EZR software Ver. 1.42 (31). The error bars in all figures represent the mean ± SD. In the subcutaneous xenograft model, repeated-measures ANOVA was applied to evaluate the statistical differences. ANOVA with Tukey's multiple comparison test was used to investigate the changes in tumor weight in the orthotopic xenograft model. Repeated-measures ANOVA was used to compare the bioluminescence intensities in the peritoneal dissemination model. A log-rank test of Kaplan-Meier curves for pairwise comparisons was performed to analyze the statistical difference in the peritoneal dissemination model. The Bonferroni's test was applied as P-value adjustment method.

Results

Preparation of anti-TF ADC. The valine-citrulline linker was adopted, as shown in Fig. 1A. The drug antibody ratios of control ADC and anti-TF ADC were determined to be 3.5 and 3.6, respectively. To evaluate the changes in molecular size between mAbs and ADCs, the particle size of each mAb and ADC was measured using a method based on PCS and DLS. The particle sizes of control mAb, control ADC, anti-TF mAb, and anti-TF ADC were 13.0±4.7, 13.0±5.2, 13.0±3.3 and 12.0±2.4 nm, respectively (Fig. 1B). These results indicated that there were no significant changes in molecular size between mAbs and ADCs. In addition, ELISA was performed to estimate the binding affinity of each mAb and ADC to recombinant human and mouse TF antigen (Fig. 1C). Anti-TF mAb and anti-TF ADC showed almost equivalent affinities to recombinant human TF antigen. However, neither reacted with recombinant mouse TF antigen. On the other hand, control mAb and control ADC did not recognize either recombinant human or mouse TF antigen. Before evaluating cytotoxic activity, TF expression was determined by performing FCM analysis using human pancreatic cancer cell lines, including Panc-1, Suit-2, PSN-1, BxPC-3 and HPAF-II (Fig. 1D). Of these, BxPC-3 and HPAF-II cells showed the highest TF antigen expression. To clarify whether the cytotoxic activity of anti-TF ADC depended on cellular TF expression, BxPC-3-TF-KO cells that did not express TF antigen on the cell surface were prepared. These three cell lines (BxPC-3, BxPC-3-TF-KO and HPAF-II) were used for the subsequent experiments.

WST-8 assays were performed to investigate the cytotoxic activity of each agent (Fig. 1E-G). The results showed that the cytotoxic effects of anti-TF ADC and MMAE were almost the same against TF-positive cells, BxPC-3 cells and HPAF-II cells (Fig. 1E and G). On the other hand, TF-negative cells, BxPC-3-TF-KO, were damaged by MMAE but not by anti-TF ADC (Fig. 1F). Control ADC had no cytotoxic activity against any of the three cell lines. In this assay, the IC_{50} values of MMAE and anti-TF ADC against BxPC-3 cells were 0.25±0.00 nM (as the ADC equivalent) and 0.25±0.02 nM, respectively (Fig. 1E). The IC_{50} value of MMAE against BxPC-3-TF-KO cells was 1.48±0.71 nM (as the ADC equivalent) (Fig. 1F). The IC_{50} values of MMAE and anti-TF ADC against HPAF-II cells were 0.06±0.01 nM (as the ADC equivalent) and 0.04±0.02 nM, respectively (Fig. 1G).

Antitumor effects in the subcutaneous tumor models. Our study next examined the antitumor effects of anti-TF ADC in three subcutaneous xenograft models. In the BxPC-3 xenograft model, no antitumor effects were observed with anti-TF mAb

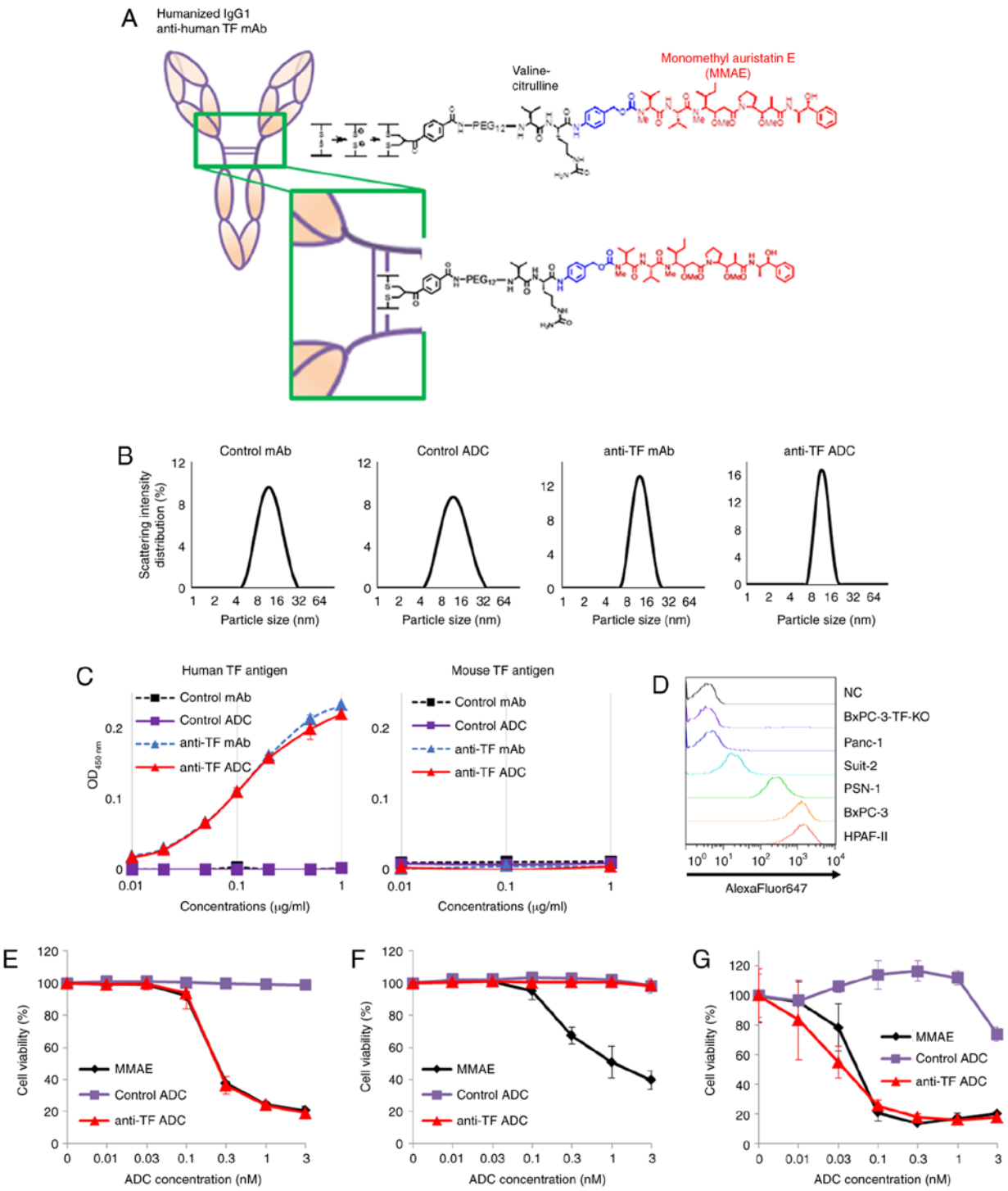

Figure 1. Preparation of humanized anti-TF ADC. (A) Diagram of the conjugation method and the chemical structure of the linker and payload. (B) Particle size of each mAb and ADC. (C) ELISA data (n=3) of each mAb or ADC against human TF antigen (left) and mouse TF antigen (right). (D) TF expression in various human pancreatic cancer cell lines according to flow cytometric analysis. Cytotoxic activity of MMAE, control ADC, and anti-TF ADC against (E) BxPC-3, (F) BxPC-3-TF-KO and (G) HPAF-II cells (n=3). TF, tissue factor; ADC, antibody-drug conjugate; mAb, monoclonal antibody; MMAE, monomethyl auristatin E; KO, knock-out.

or control ADC (Fig. 2A). Our previous reports also confirmed that the rat anti-TF mAb (IgG2b) by itself did not show an antitumor effect *in vivo* (19,22).

In the present study, humanized anti-TF mAb (IgG1) was prepared, which was expected to exert an antibody-dependent cellular cytotoxicity effect *in vivo*; however, it did not have an antitumor effect. On the other hand, anti-TF ADC showed a significant antitumor effect (Fig. 2A). Anti-TF ADC at doses of 2, 5 and 10 mg/kg exhibited significantly greater antitumor effects than those of control ADC at 10 mg/kg ($P<0.005$, $P<0.001$ and $P<0.001$, respectively). The antitumor effects of anti-TF ADC were clearly dose dependent. In the BxPC-3-TF-KO xenograft model, anti-TF ADC did not inhibit tumor growth any more than DPBS ($P=0.997$),

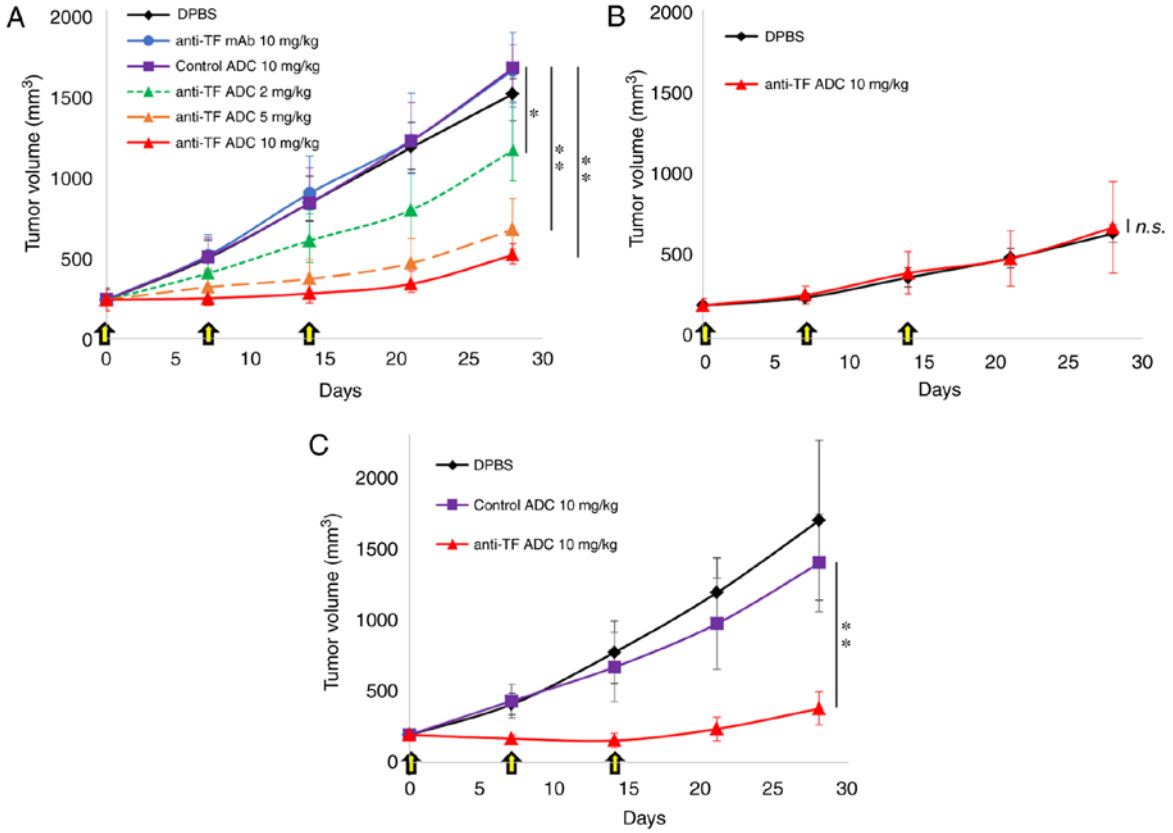

Figure 2. *In vivo* antitumor effect in subcutaneous xenograft models. The *in vivo* efficacy of anti-TF ADC was evaluated in nude mice bearing (A) BxPC-3, (B) BxPC-3-TF-KO and (C) HPAF-II cells. Mice were intravenously injected weekly for 3 weeks, as indicated by the arrows (n=5). Repeated-measures ANOVA was used for statistical analysis. All error bars indicate SD. *P<0.005, **P<0.001; n.s., not significant. TF, tissue factor; ADC, antibody-drug conjugate.

indicating that the effects of anti-TF ADC depended entirely on the expression of TF in tumor tissues (Fig. 2B). Furthermore, the growth speed of BxPC-3-TF-KO tumors was slower than that of BxPC-3 tumors (Fig. 2A and B), indicating that TF expression in BxPC-3 tumors contributed to accelerating tumor growth *in vivo*. In the HPAF-II xenograft model, control ADC did not show an antitumor effect, whereas anti-TF ADC caused tumor shrinkage (Fig. 2C). Statistically, there was a significant difference between treatment with control ADC at 10 mg/kg and anti-TF ADC at 10 mg/kg (P<0.001). Although tumor growth was inhibited during treatment with anti-TF ADC (10 mg/kg) in the BxPC-3 and HPAF-II xenograft models, tumor regrowth was observed after the end of treatment in both models (Fig. 2A and C). There were no body weight changes in the mice treated with anti-TF ADC in the subcutaneous tumor models (Fig. S1A-C).

Antitumor effects in the orthotopic tumor models. Our study examined the antitumor effects of anti-TF ADC in an orthotopic xenograft model using the treatment schedule shown in Fig. 3A. After treatment with DPBS or 10/mg/kg anti-TF ADC or control ADC, each tumor was resected (Fig. 3B). Tumor weights are plotted in Fig. 3C. The tumors treated with anti-TF ADC weighed significantly less than those treated with DPBS or control ADC (P<0.001). These results indicate that anti-TF ADC efficiently delivered the payload to the pancreatic tumor and inhibited tumor growth in the orthotopic pancreatic tumor model. Body weight changes of mice were not observed in the orthotopic xenograft model (Fig. S1D).

Antitumor effects in a peritoneal dissemination model. The antitumor effect of anti-TF ADC was evaluated in a pancreatic cancer peritoneal dissemination model. One week after implantation of HPAF-II-Luc cells into the abdominal cavity of mice, the bioluminescence intensity of the abdominal area of the mice was measured, and the animals were randomly grouped (Day 0). The bioluminescence intensity of each mouse was measured at Day 14 and 28. The bioluminescence images of each mouse are shown in Fig. 4A. In the group treated with DPBS at Day 28, images of three mice could not be obtained due to prior tumor-related death. Also, the bioluminescence intensity at each time point was plotted (Fig. 4B). The mice treated with anti-TF ADC showed significantly lower bioluminescence intensity than that exhibited by the mice treated with DPBS or control ADC (P<0.001 both). Hence, anti-TF ADC inhibited tumor growth in the abdominal cavity in this model. On the other hand, widespread dissemination occurred in the mice treated with DPBS or control ADC. It is notable that, in mice with peritoneal dissemination, the antitumor effect of anti-TF ADC extended the survival time compared with that caused by DPBS (P=0.000017) and control ADC (P=0.000011) (Fig. 4C). In this experiment, the treatments with anti-TF ADC did not affect the body weight change of mice (Fig. S1E).

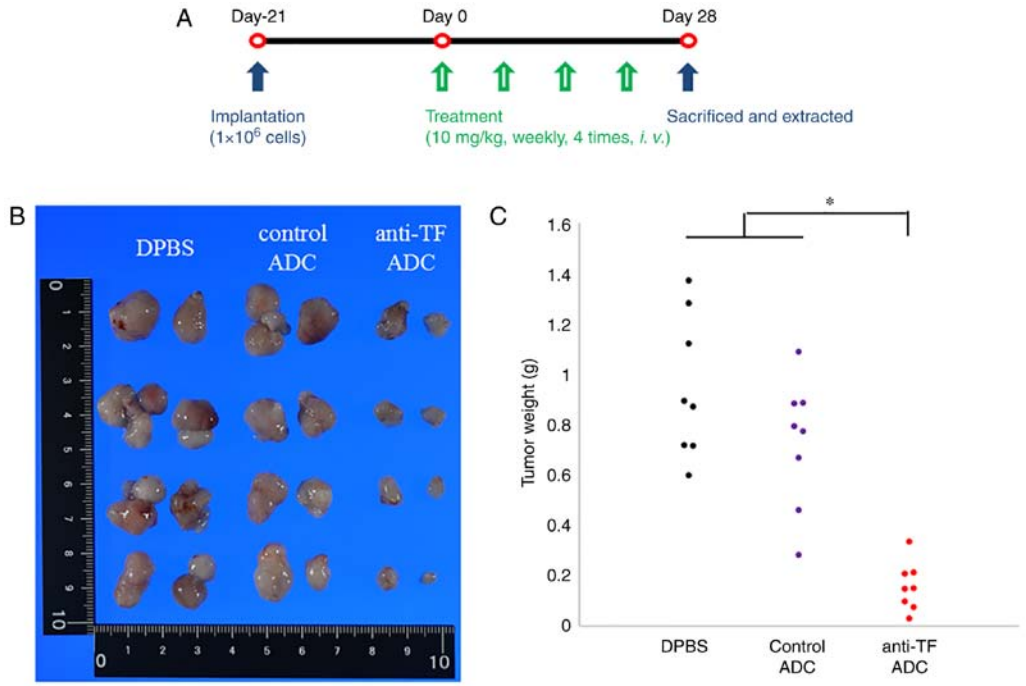

Figure 3. *In vivo* antitumor effect in orthotopic xenograft model. (A) Experimental schedule. (B) Tumors resected from mice intravenously treated with DPBS, control ADC (10 mg/kg), or anti-TF ADC (10 mg/kg) (n=8). (C) Weights of the resected tumors (n=8). ANOVA with Tukey's multiple comparison test was used for statistical analysis. *P<0.001. TF, tissue factor; ADC, antibody-drug conjugate; i.v., intravenously.

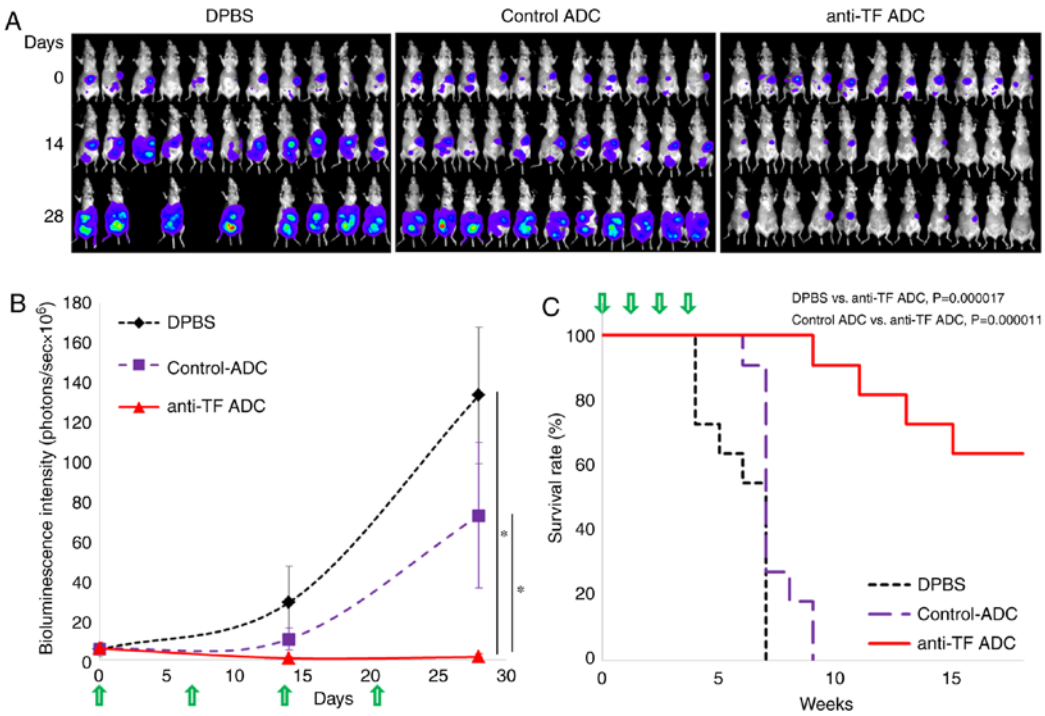

Figure 4. *In vivo* antitumor effect in a peritoneal dissemination model. (A) Bioluminescence images of mice intravenously treated with DPBS, control ADC (10 mg/kg), or anti-TF ADC (10 mg/kg) (n=11). (B) Bioluminescence intensity of each mouse (n=11). Repeated-measures ANOVA was used for statistical analysis. *P<0.001. Error bars represent SD. (C) Kaplan-Meier curve in the survival study (n=11). The log-rank test for pairwise comparisons showed the statistical differences between the mice treated with DPBS and anti-TF ADC (P=0.000017), and that with control ADC and anti-TF ADC (P=0.000011). Arrows indicate the administration of DPBS and both ADCs. TF, tissue factor; ADC, antibody-drug conjugate.

Discussion

Currently, numerous antibody-drug conjugates (ADCs) have been investigated in clinical trials. Since tissue factor (TF) expression has been observed in a wide range of solid tumors, anti-TF ADC is also expected to be a promising cancer treatment. Phase 1 and 2 clinical trials of tisotumab vedotin were conducted in patients with advanced metastatic solid

cancer (InnovaTV 201) (24,25). In these studies, the authors demonstrated that tisotumab vedotin had a manageable safety profile and a preliminary antitumor effect. A different group developed anti-TF ADCs other than tisotumab vedotin, and showed that one anti-TF ADC did not affect blood coagulation (17,21). Our group also established several rat anti-TF mAb clones and compared their characteristics (19,22,32). Our experiments indicated that mAb clone 1084 had suitable characteristics for ADC design. Although ADC 1084 had a higher binding affinity constant (K_D) and higher dissociation constant rate (k_d) than those of other anti-TF ADCs, it was able to penetrate more deeply into tumor clusters and exerted a greater antitumor effect in large-sized tumors (approximately 600 mm^3) in the pancreatic cancer xenograft model. Since another report demonstrated that TF is efficient and rapidly turned over on TF-positive tumor cells (20), it was hypothesized that the change in k_d may not affect the internalization efficiency of anti-TF ADCs, but may instead have an effect on tumor-penetration ability. In the present study, therefore, a humanized anti-TF mAb was established from rat anti-TF mAb (clone 1084) and humanized anti-TF ADC was prepared for cancer treatment.

The present study successfully produced humanized anti-TF ADC that was able to bind to human TF antigens, but not to mouse TF antigens. The WST-8 assay *in vitro* demonstrated that anti-TF ADC showed high cytotoxic activity against two TF-positive pancreatic cancer cell lines, namely BxPC-3 and HPAF-II, but not against the BxPC-3-TF-KO cell line, which is TF-negative. In subcutaneous xenograft models, anti-TF ADC also exhibited a high antitumor effect in BxPC-3 and HPAF-II tumors, but not in BxPC-3-TF-KO tumors. Additionally, anti-TF ADC efficiently delivered the anticancer agent to orthotopic tumors, whose microenvironments may be more similar to that of clinical pancreatic cancer than to that of subcutaneous tumors, and exerted an antitumor effect in the orthotopic model. Furthermore, anti-TF ADC significantly extended the survival period in the peritoneal dissemination mouse model, in which mice with no treatment showed a shorter survival time (approximately 2 months) due to tumor dissemination in the abdominal region. These results indicated that anti-TF ADC has the potential to be an efficacious treatment not only for primary tumors but also for tumors that have widely disseminated. In future studies, other metastatic tumor models such as a liver metastatic tumor model would be useful to evaluate the efficacy of anti-TF ADC in advanced pancreatic cancer. Furthermore, although a bleeding risk due to the use of tisotumab vedotin was reported as manageable in the clinical study (24,25), our present humanized anti-TF ADC should be carefully evaluated for these potential adverse events and distribution in normal tissues in the appropriate models.

As mentioned above, there have been several reports on anti-TF ADCs. All of them, including tisotumab vedotin, adopted the valine-citrulline linker and used microtubule inhibitors such as MMAE and MMAF as the payload. Although MMAE has been used in a number of ADCs, other payloads (e.g., DNA-damaging agents) have also demonstrated *in vivo* efficacy (33,34). Furthermore, multiple studies revealed that cancer cells can develop resistance to ADCs conjugated with MMAE because MMAE can be pumped out of the cell via transporters (e.g., P-glycoprotein) (35-37). Therefore, other payloads are expected to be investigated for the design of anti-TF ADCs in order to increase their efficacy.

Acknowledgements

The authors would like to thank Ms. M Shimada at the National Cancer Center, Japan for her secretarial help.

Funding

The research was supported by the National Cancer Center Research and Development Fund (23-A-45 and 29-A-9 to YM) and by the Japan Society for the Promotion of Science (JSPS) KAKENHI Grant Number JP 18K14931 and 20K16021 (to RT).

Availability of data and materials

All data generated during this study are available from the corresponding author on reasonable request.

Authors' contributions

RT mainly performed the *in vitro* and *in vivo* experiments. TA was involved in the production and the preparation of the humanized antibody. SM was involved in the preparation of the linker compound. HT was involved in the preparation of tissue factor antigen for ELISA. RT, YK, MY and YM contributed to the study conception and design. RT and YM drafted the manuscript. All authors have read and approved the final manuscript.

Ethics approval and consent to participate

All animal experiments were carried out with the approval of the Committee for Animal Experimentation of the National Cancer Center, Japan. Experiments met the ethical standards required by law and also complied with guidelines for the use of experimental animals in Japan.

Patient consent for publication

Not applicable.

Competing interests

The authors declare that they have no competing interests.

References

1. Howlader N, Noone AM, Krapcho M, Miller D, Bishop K, Kosary CL, Yu M, Ruhl J, Tatalovich Z, Mariotto A, *et al* (eds): SEER Cancer Statistics Review. 1975-2014, National Cancer Institute Bethesda, MD, https://seercancergov/csr/1975_2014/, based on November 2016 SEER data submission, posted to the SEER web site, April 2017. Accessed May 11, 2017.
2. Rhim AD, Mirek ET, Aiello NM, Maitra A, Bailey JM, McAllister F, Reichert M, Beatty GL, Rustgi AK, Vonderheide RH, *et al*: EMT and dissemination precede pancreatic tumor formation. Cell 148: 349-361, 2012.

3. Ferrone CR, Pieretti-Vanmarcke R, Bloom JP, Zheng H, Szymonifka J, Wargo JA, Thayer SP, Lauwers GY, Deshpande V, Mino-Kenudson M, *et al*: Pancreatic ductal adenocarcinoma: Long-term survival does not equal cure. Surgery 152 (3 Suppl 1): S43-S49, 2012.
4. Khorana AA and Fine RL: Pancreatic cancer and thromboembolic disease. Lancet Oncol 5: 655-663, 2004.
5. Rak J, Yu JL, Luyendyk J and Mackman N: Oncogenes, trousseau syndrome, and cancer-related changes in the coagulome of mice and humans. Cancer Res 66: 10643-10646, 2006.
6. Stein PD, Beemath A, Meyers FA, Skaf E, Sanchez J and Olson RE: Incidence of venous thromboembolism in patients hospitalized with cancer. Am J Med 119: 60-68, 2006.
7. Matsumura Y: Cancer stromal targeting (CAST) therapy. Adv Drug Deliv Rev 64: 710-719, 2012.
8. Callander NS, Varki N and Rao LV: Immunohistochemical identification of tissue factor in solid tumors. Cancer 70: 1194-1201, 1992.
9. Nitori N, Ino Y, Nakanishi Y, Yamada T, Honda K, Yanagihara K, Kosuge T, Kanai Y, Kitajima M and Hirohashi S: Prognostic significance of tissue factor in pancreatic ductal adenocarcinoma. Clin Cancer Res 11: 2531-2539, 2005.
10. van den Berg YW, Osanto S, Reitsma PH and Versteeg HH: The relationship between tissue factor and cancer progression: Insights from bench and bedside. Blood 119: 924-932, 2012.
11. Kasthuri RS, Taubman MB and Mackman N: Role of tissue factor in cancer. J Clin Oncol 27: 4834-4838, 2009.
12. Bourcy M, Suarez-Carmona M, Lambert J, Francart ME, Schroeder H, Delierneux C, Skrypek N, Thompson EW, Jerusalem G, Berx G, *et al*: Tissue factor induced by epithelial-mesenchymal transition triggers a procoagulant state that drives metastasis of circulating tumor cells. Cancer Res 76: 4270-4282, 2016.
13. Hisada Y and Mackman N: Tissue factor and cancer: Regulation, tumor growth, and metastasis. Semin Thromb Hemost 45: 385-395, 2019.
14. Yamashita H, Kitayama J, Ishikawa M and Nagawa H: Tissue factor expression is a clinical indicator of lymphatic metastasis and poor prognosis in gastric cancer with intestinal phenotype. J Surg Oncol 95: 324-331, 2007.
15. Sawada M, Miyake S, Ohdama S, Matsubara O, Masuda S, Yakumaru K and Yoshizawa Y: Expression of tissue factor in non-small-cell lung cancers and its relationship to metastasis. Br J Cancer 79: 472-477, 1999.
16. Versteeg HH, Schaffner F, Kerver M, Petersen HH, Ahamed J, Felding-Habermann B, Takada Y, Mueller BM and Ruf W: Inhibition of tissue factor signaling suppresses tumor growth. Blood 111: 190-199, 2008.
17. Zhang X, Li Q, Zhao H, Ma L, Meng T, Qian J, Jin R, Shen J and Yu K: Pathological expression of tissue factor confers promising antitumor response to a novel therapeutic antibody SC1 in triple negative breast cancer and pancreatic adenocarcinoma. Oncotarget 8: 59086-59102, 2017.
18. Breij EC, de Goeij BE, Verploegen S, Schuurhuis DH, Amirkhosravi A, Francis J, Miller VB, Houtkamp M, Bleeker WK, Satijn D and Parren PW: An antibody-drug conjugate that targets tissue factor exhibits potent therapeutic activity against a broad range of solid tumors. Cancer Res 74: 1214-1226, 2014.
19. Koga Y, Manabe S, Aihara Y, Sato R, Tsumura R, Iwafuji H, Furuya F, Fuchigami H, Fujiwara Y, Hisada Y, *et al*: Antitumor effect of antitissue factor antibody-MMAE conjugate in human pancreatic tumor xenografts. Int J Cancer 137: 1457-1466, 2015.
20. de Goeij BE, Satijn D, Freitag CM, Wubbolts R, Bleeker WK, Khasanov A, Zhu T, Chen G, Miao D, van Berkel PH and Parren PW: High turnover of tissue factor enables efficient intracellular delivery of antibody-drug conjugates. Mol Cancer Ther 14: 1130-1140, 2015.
21. Theunissen JW, Cai AG, Bhatti MM, Cooper AB, Avery AD, Dorfman R, Guelman S, Levashova Z and Migone TS: Treating tissue factor-positive cancers with antibody-drug conjugates that do not affect blood clotting. Mol Cancer Ther 17: 2412-2426, 2018.
22. Tsumura R, Manabe S, Takashima H, Koga Y, Yasunaga M and Matsumura Y: Influence of the dissociation rate constant on the intra-tumor distribution of antibody-drug conjugate against tissue factor. J Control Release 284: 49-56, 2018.
23. Tsumura R, Manabe S, Takashima H, Koga Y, Yasunaga M and Matsumura Y: Evaluation of the antitumor mechanism of antibody-drug conjugates against tissue factor in stroma-rich allograft models. Cancer Sci 110: 3296-3305, 2019.
24. Hong DS, Concin N, Vergote I, de Bono JS, Slomovitz BM, Drew Y, Arkenau HT, Machiels JP, Spicer JF, Jones R, *et al*: Tisotumab vedotin in previously treated recurrent or metastatic cervical cancer. Clin Cancer Res 26: 1220-1228, 2020.
25. de Bono JS, Concin N, Hong DS, Thistlethwaite FC, Machiels JP, Arkenau HT, Plummer R, Jones RH, Nielsen D, Windfeld K, *et al*: Tisotumab vedotin in patients with advanced or metastatic solid tumours (InnovaTV 201): A first-in-human, multicentre, phase 1-2 trial. Lancet Oncol 20: 383-393, 2019.
26. Badescu G, Bryant P, Bird M, Henseleit K, Swierkosz J, Parekh V, Tommasi R, Pawlisz E, Jurlewicz K, Farys M, *et al*: Bridging disulfides for stable and defined antibody drug conjugates. Bioconjug Chem 25: 1124-1136, 2014.
27. Bryant P, Pabst M, Badescu G, Bird M, McDowell W, Jamieson E, Swierkosz J, Jurlewicz K, Tommasi R, Henseleit K, *et al*: In vitro and in vivo evaluation of cysteine rebridged trastuzumab-MMAE antibody drug conjugates with defined drug-to-antibody ratios. Mol Pharm 12: 1872-1879, 2015.
28. Yasunaga M, Saijou S, Hanaoka S, Anzai T, Tsumura R and Matsumura Y: Significant antitumor effect of an antibody against TMEM180, a new colorectal cancer-specific molecule. Cancer Sci 110: 761-770, 2019.
29. Kuramochi T, Igawa T, Tsunoda H and Hattori K: Humanization and simultaneous optimization of monoclonal antibody. Methods Mol Biol 1060: 123-137, 2014.
30. Tsumura R, Sato R, Furuya F, Koga Y, Yamamoto Y, Fujiwara Y, Yasunaga M and Matsumura Y: Feasibility study of the Fab fragment of a monoclonal antibody against tissue factor as a diagnostic tool. Int J Oncol 47: 2107-2114, 2015.
31. Kanda Y: Investigation of the freely available easy-to-use software 'EZR' for medical statistics. Bone Marrow Transplant 48: 452-458, 2013.
32. Saito Y, Hashimoto Y, Kuroda J, Yasunaga M, Koga Y, Takahashi A and Matsumura Y: The inhibition of pancreatic cancer invasion-metastasis cascade in both cellular signal and blood coagulation cascade of tissue factor by its neutralisation antibody. Eur J Cancer 47: 2230-2239, 2011.
33. Jeffrey SC, Burke PJ, Lyon RP, Meyer DW, Sussman D, Anderson M, Hunter JH, Leiske CI, Miyamoto JB, Nicholas ND, *et al*: A potent anti-CD70 antibody-drug conjugate combining a dimeric pyrrolobenzodiazepine drug with site-specific conjugation technology. Bioconjug Chem 24: 1256-1263, 2013.
34. Ogitani Y, Aida T, Hagihara K, Yamaguchi J, Ishii C, Harada N, Soma M, Okamoto H, Oitate M, Arakawa S, *et al*: DS-8201a, a novel HER2-targeting ADC with a Novel DNA topoisomerase I inhibitor, demonstrates a promising antitumor efficacy with differentiation from T-DM1. Clin Cancer Res 22: 5097-5108, 2016.
35. Chen R, Hou J, Newman E, Kim Y, Donohue C, Liu X, Thomas SH, Forman SJ and Kane SE: CD30 downregulation, MMAE resistance, and MDR1 upregulation are all associated with resistance to brentuximab vedotin. Mol Cancer Ther 14: 1376-1384, 2015.
36. Yu SF, Zheng B, Go M, Lau J, Spencer S, Raab H, Soriano R, Jhunjhunwala S, Cohen R, Caruso M, *et al*: A novel anti-CD22 anthracycline-based antibody-drug conjugate (ADC) that overcomes resistance to auristatin-based ADCs. Clin Cancer Res 21: 3298-3306, 2015.
37. Liu-Kreyche P, Shen H, Marino AM, Iyer RA, Humphreys WG and Lai Y: Lysosomal P-gp-MDR1 confers drug resistance of brentuximab vedotin and its cytotoxic payload monomethyl auristatin e in tumor cells. Front Pharmacol 10: 749, 2019.